Molecular mechanisms underlying the exceptional adaptations of batoid fins

Tetsuya Nakamura[a], Jeff Klomp[a], Joyce Pieretti[a], Igor Schneider[b], Andrew R. Gehrke[a], and Neil H. Shubin[a,1]

[a]Department of Organismal Biology and Anatomy, University of Chicago, Chicago, IL 60637; and [b]Instituto de Ciencias Biologicas, Universidade Federal do Para, 66075 Belem, Brazil

Contributed by Neil H. Shubin, November 5, 2015 (sent for review September 18, 2015; reviewed by Karen D. Crow and Clifford J. Tabin)

Extreme novelties in the shape and size of paired fins are exemplified by extinct and extant cartilaginous and bony fishes. Pectoral fins of skates and rays, such as the little skate (Batoid, *Leucoraja erinacea*), show a strikingly unique morphology where the pectoral fin extends anteriorly to ultimately fuse with the head. This results in a morphology that essentially surrounds the body and is associated with the evolution of novel swimming mechanisms in the group. In an approach that extends from RNA sequencing to in situ hybridization to functional assays, we show that anterior and posterior portions of the pectoral fin have different genetic underpinnings: canonical genes of appendage development control posterior fin development via an apical ectodermal ridge (AER), whereas an alternative *Homeobox* (*Hox*)–*Fibroblast growth factor* (*Fgf*)–*Wingless type MMTV integration site family* (*Wnt*) genetic module in the anterior region creates an AER-like structure that drives anterior fin expansion. Finally, we show that *GLI family zinc finger 3* (*Gli3*), which is an anterior repressor of tetrapod digits, is expressed in the posterior half of the pectoral fin of skate, shark, and zebrafish but in the anterior side of the pelvic fin. Taken together, these data point to both highly derived and deeply ancestral patterns of gene expression in skate pectoral fins, shedding light on the molecular mechanisms behind the evolution of novel fin morphologies.

skate | fin | evolution | development | AER

The paired fins of fishes are extraordinarily diverse in skeletal composition, pattern, and function (1–3) (Fig. 1*A*). In particular, the cartilaginous fishes (chimaeras, sharks, skates, and rays) exhibit morphological variation in appendages, such as claspers in males and extreme elongation in the caudal fin of thresher sharks. Batoids (skates and rays) exhibit an extraordinarily modified body plan that is dorso-ventrally flattened, with a novel pectoral fin morphology that is unique among vertebrates. The pectoral fins extend anteriorly and fuse with the head, establishing a broad wing and flat body adapted to benthic life (4, 5). This remarkable appendage is composed of three basal cartilages, the propterygium, mesopterygium, and metapterygium, which extend along the anterior–posterior (A–P) axis to support the fin. Although ancestral fishes have these three bones, they are significantly shorter compared with skate (Fig. 1*A*).

Although a great deal is known about the molecular mechanisms that build tetrapod limbs, significantly less is known about the genetic underpinnings of appendage diversity in vertebrates more broadly. Previous studies of skate development have revealed a constellation of ancestral and derived traits (5, 6). The paired fin buds of skates initiate development in the same lateral position of the body as observed in the shark, however the width of the fin buds along the A–P axis is wider than other fishes (5). During later development, the pectoral fin dramatically transforms its shape, extending anteriorly. As in tetrapods, *Sonic hedgehog* (*Shh*) expression is detected in a restricted posterior domain in the developing fins of the little skate *Leucoraja erinacea* (7) as well as the developing clasper (8). Although equivalent expression patterns of *5′Hox* genes are found in paired fins/limbs of sharks and tetrapods (9), there are some differences in the A–P expression of key factors. For example, *Gli3* mRNA is more enriched in the posterior pectoral fins of fishes as opposed to the anterior region in tetrapods (10). It remains unknown how the skate embryo extends the anterior fin domain, where no *Shh* transcripts are detected, and whether the SHH–Fibroblast Growth Factor (FGF)–Homeobox (HOX) signaling axis drives anterior fin growth.

To address the molecular mechanisms of fin diversity, we have performed a functional genomic screen during fin development of the little skate, *L. erinacea*. Using multiple approaches extending from RNA sequencing (RNA-seq) and in situ hybridization to functional assays, we show that anterior and posterior portions of paired fins have different genetic underpinnings within the little skate and among vertebrates. Canonical genes of appendage development control the posterior fin development in skate, whereas an alternative *Hox–Fgf–Wingless type MMTV integration site family* (*Wnt*) genetic module in the anterior region creates a second apical ectodermal ridge (AER) that is likely to drive anterior fin expansion.

Results

RNA-seq in the Skate Pectoral Fin. During pectoral fin development in skates, the anterior portion of the fin elongates along the A–P axis (Fig. 1 *B–E* and *SI Appendix*, Fig. S1). To identify the profile of genes expressed at different times and places during skate fin development, we conducted RNA-seq on three portions of the pectoral fin (anterior, central, and posterior) at three different stages (stages 29, 30, and 31) (Fig. 2*A* and *SI Appendix*, Fig. S2).

Significance

With pectoral fins that surround much of the body, by fusing to the head, the skate is a cartilaginous fish that has one of the most unique appendages of all vertebrates. Here, we use an unbiased RNA screen to uncover genetic pathways underlying this morphology. Unlike tetrapods and other fishes, skates induce a second growth center in the anterior region, by the redeployment of an ancient genetic module. We find that some of the genes involved in generating the anterior–posterior fin function differently in skates than they do in limbed animals. Our data reveal the mechanisms for the unique skate fin morphology and also provide insights into the genetic origins of fin variation and morphological innovation in paired appendages.

Author contributions: T.N. and J.P. designed research; T.N. and J.P. performed research; T.N., J.K., J.P., I.S., A.R.G., and N.H.S. analyzed data; and T.N., J.K., J.P., I.S., A.R.G., and N.H.S. wrote the paper.

Reviewers: K.D.C., San Francisco State University; and C.J.T., Harvard Medical School.

The authors declare no conflict of interest.

Freely available online through the PNAS open access option.

Data deposition: The sequences reported in this paper (*S. rotifer Hoxa5 and C. plagiosum Gli3*) have been deposited in the GenBank database (accession nos. KT425371 and KT425372). Transcriptome sequencing data have been deposited at the National Center for Biotechnology Information Sequence Read Archives (NCBI SRA), www.ncbi.nlm.nih.gov/sra (BioProject accession code PRJNA288370).

[1]To whom correspondence should be addressed. Email: nshubin@uchicago.edu.

This article contains supporting information online at www.pnas.org/lookup/suppl/doi:10.1073/pnas.1521818112/-/DCSupplemental.

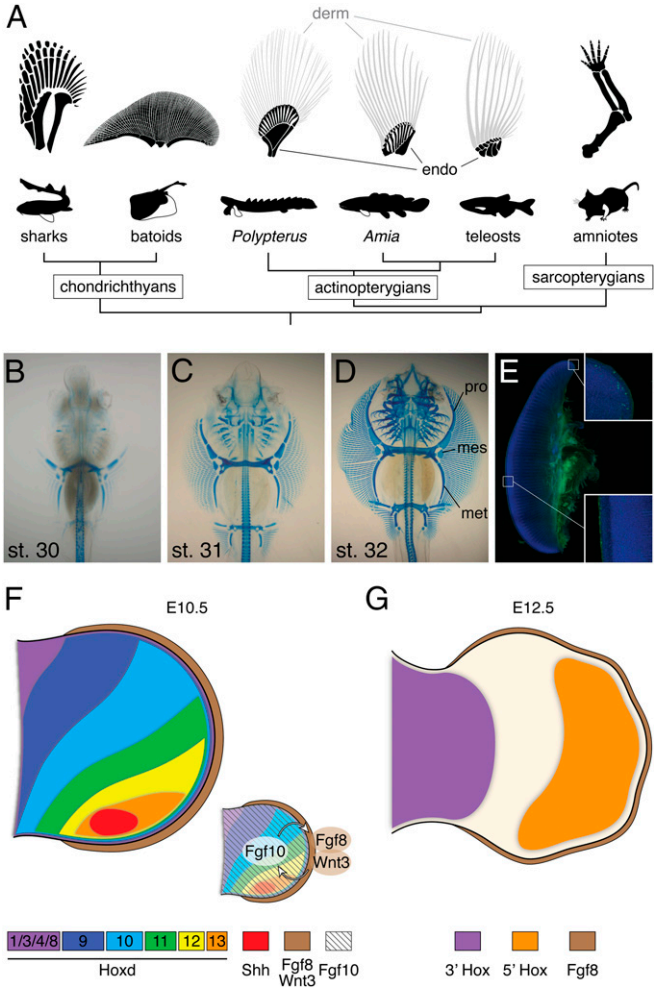

Fig. 1. Appendage diversity and the skate unique fin. (*A*) The pectoral fin and forelimb skeleton in a variety of taxa. Chondrichthyan and basal actinopterygian fins are composed of three bones, pro-, meso-, and metapterygium, whereas the sarcopterygian appendage is a single rod of the metapterygium axis. The batoid fin is extremely wide along the A–P axis compared with other vertebrates. Dermal bones (derm) and endochondral bones (endo) are labeled by gray and black colors depending on the difference of its developmental mechanisms (36). (*B–D*) Alcian Blue-stained skeletal preparations of skate embryos at stages 30–32. mes, mesopterygium; met, metapterygium; pro, propterygium. Both pectoral and pelvic fins elongate along the A–P axis. (*E*) Immunostaining for phosphorylated histone H3 (green) and DAPI (blue) in the pectoral fin at stage 31. Image composed using tiled scanning by confocal microscope (Zeiss ZEN software). *Inset*, magnified portions of the anterior and central fin. Statistical analysis of cell proliferation rates in each portion can be found in *SI Appendix*, Fig. S1. (*F* and *G*) Summary of the developmental mechanisms of the tetrapod limb. At an early stage (*F*), *Shh* is expressed in the posterior limb bud, and *5′Hox* genes show a gradient of expression. *Fgf10* induces and maintains AER structure. In turn, *Fgf8* and *Wnt3* in AER stimulate cell proliferation in the limb mesenchyme. As the limb bud develops, *5′Hox* genes mark the autopod domain, whereas *3′Hox* genes are expressed in the proximal limb.

In lieu of a skate genome, each mRNA was annotated using the zebrafish genome. RNA-seq identified *Alx4* and *Pax9* (known anterior-specific limb genes in tetrapods) (11, 12) in the anterior pectoral fin, indicating the efficacy of this technique to identify site-specific gene activity (Fig. 2*A*). RNA-seq also revealed a number of genes that were significantly enriched in the posterior portion of the fin (Fig. 2 *A* and *B*). These include genes involved in the limb development, including *Hox*, *Fgf*, and *Wnt*. We performed in situ hybridization of a subset of these genes to characterize their expression patterns. *Fgf8–Fgf10*, which maintain the AER and stimulate cell proliferation in tetrapod limbs (Fig. 1 *F* and *G*) (13, 14), are expressed in the posterior half of the fin (Fig. 2 *A–D*). *Fgf8* expression is restricted to the posterior ectoderm, whereas *Fgf10* is expressed in the posterior mesenchyme (Fig. 2 *C* and *D*). The *5′Hox* genes also localize in the posterior fin, consistent with the pattern described in limbs (Fig. 2 *A*, *B*, and *F–H*). These data demonstrate that the mechanisms for maintaining the posterior fin development in skate are equivalent to those of the tetrapod limb.

Anterior Extension During Skate Fin Development. To investigate the embryological development of the skate fin's anterior extension, we performed whole-mount fin staining for the cell proliferation marker phosphorylated histone H3. Initially, the staining pattern showed uniform distribution of fluorescent nuclei at stage 29. Later in fin development, the number of positive cells increased in both anterior and posterior regions of the fin (stage 31) (Fig. 1*E* and *SI Appendix*, Fig. S1), indicating that skate fin elongation consists of two domains of enriched cell proliferation.

RNA-seq showed that *Wnt3*, which maintains the AER in limb development (Fig. 1*F*) (15–19), is expressed in both the anterior and posterior fin compartments (Fig. 2*B*). Whole-mount in situ hybridization showed that *Wnt3* is expressed in the fin ectoderm at stage 29 and continues to be expressed in the posterior tip at stage 30 (Fig. 3*C* and *SI Appendix*, Fig. S3). Surprisingly, and in concordance with the RNA-seq results, we found that *Wnt3* is also expressed in the anterior ectoderm at stage 30 (Fig. 3*B* and *SI Appendix*, Fig. S10*A*). In addition, *Bmp4*, a secreted factor and indispensable to the maintenance of the AER (20), is highly expressed in the anterior and posterior fin, whereas *Bmp2* is localized to the posterior fin (*SI Appendix*, Fig. S10 *D* and *E*). Furthermore, sagittal sections of skate fins showed that there is a thickened ectodermal tissue in the anterior pectoral fin, similar to the AER structure (Fig. 3 *F* and *G*). As *Wnt3* maintains the AER in tetrapod limbs, we hypothesized that the anterior expression in skate fins could represent a mechanism for anterior fin elongation. To test the function of *Wnt3* in the developing skate fins, we added an inhibitor of the canonical WNT signaling pathway (IWR-1) (21) directly to their aquarium seawater at stage 24. After 3 weeks of development under these conditions, we assessed alterations to the fin skeleton using Alcian Blue staining (Fig. 3 *D* and *E*). In WNT-inhibited fins, the propterygium of the pectoral and pelvic fins were shorter than control embryos and notably did not elongate anteriorly. In addition, the metapterygium was also slightly reduced. These results suggest that the anterior skate fin extends along an A–P axis through the establishment of a proliferative region that resembles a second AER.

A Deployment of *3′Hox* and *Fgf7* Module for Anterior Extension. To identify the molecular mechanisms responsible for maintaining the anterior AER-like tissue, we again turned to the RNA-seq results to investigate genes that are differentially expressed in the anterior fin. We found that *3′Hox* genes and *Fgf7* mRNAs were highly enriched in the anterior portion of the pectoral fin (Fig. 2 *A* and *B*). We regarded these genes as candidates for anterior fin development due to their role in morphogenesis of the tetrapod proximal limb (22). In situ hybridization and real-time PCR validated that *3′Hoxa* and *3′Hoxd* genes are highly expressed in the anterior mesenchyme at stage 30 (Figs. 4 *A–D* and *SI Appendix*, Figs. S7 and S8). To reinforce these findings phylogenetically, we investigated the pattern of *Hoxa5* expression in the bamboo shark (*Chiloscyllium plagiosum*), another cartilaginous fish. We found that *Hoxa5* is expressed, as in the skate, in the anterior and posterior (but not the center) of the pectoral fin mesenchyme of the bamboo shark embryo at stage 31 (Fig. 4*E*).

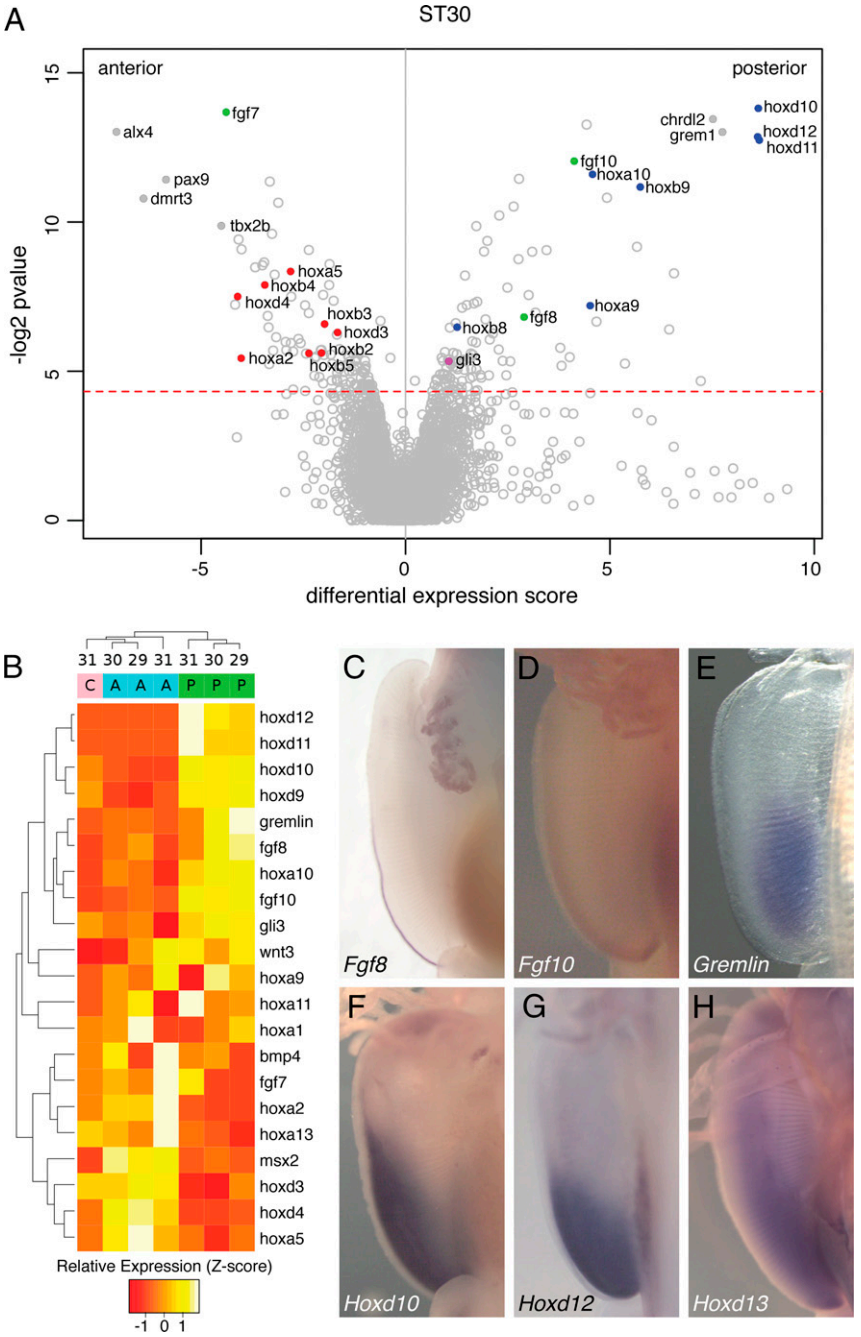

Fig. 2. Analysis of skate fin development by RNA-seq. (*A*) Differential expression of transcripts assembled from RNA-seq of anterior and posterior fin tissue specimens of stage 30 skates. Differential expression score is derived from multiple A–P comparisons of transcript abundance ($n = 3$; see *SI Appendix*). Above the red dotted line corresponds to P values less than 0.05. Blue, *5′Hox* genes; green, *Fgf* genes; purple, *Gli3*; red, *3′Hox* genes. (*B*) Standardized read counts (z-scores) for selected transcripts in the pectoral fin at three developmental stages and locations of the pectoral fin. Transcripts were median-summarized according to their annotations. A, anterior fin; C, center fin; P, posterior fin. Sample developmental stages are listed at the top, and clustering is based on relative expression levels. (*C–H*) Whole-mount in situ hybridization for canonical tool kit genes for limb development at stage 30. (*C*) *Fgf8*. The expression is at the posterior ectoderm. (*D*) *Fgf10*. The expression can be seen at the posterior mesenchyme. (*E*) *Gremlin*. (*F*) *Hoxd10*. (*G*) *Hoxd12*. (*H*) *Hoxd13*. Note that all expression patterns are limited to the posterior half, not in the anterior fin.

However, we could not detect expression of other *3′Hox* transcripts in the anterior fin of bamboo sharks. These results indicate that one of the anterior *3′Hox* expression patterns is conserved in other cartilaginous fishes and likely plays a role in fin development, but many *3′Hox* and also *Fgf7* expressions are unique in the skate pectoral fin. To explore the function of *3′Hox* genes in the establishment of an AER-like tissue, we took advantage of the native module in the zebrafish fin to overcome difficulties of genetic manipulations in skate embryos (*SI Appendix*, Fig. S9*A*). First, to decrease *Wnt3a* expression in the zebrafish fin, we treated zebrafish embryos with cyclopamine from 24–36 hours post-fertilization (hpf). Cyclopamine disrupts the *Shh-5′Hox* module, resulting in a loss of native *Wnt3a* expression in the fin (21/21 embryos; *SI Appendix*, Fig. S9 *B* and *C*). Next, we used a previously reported fin enhancer, gar Island I (23), to drive ectopic *Hoxa2b* in the distal mesenchyme of the fins

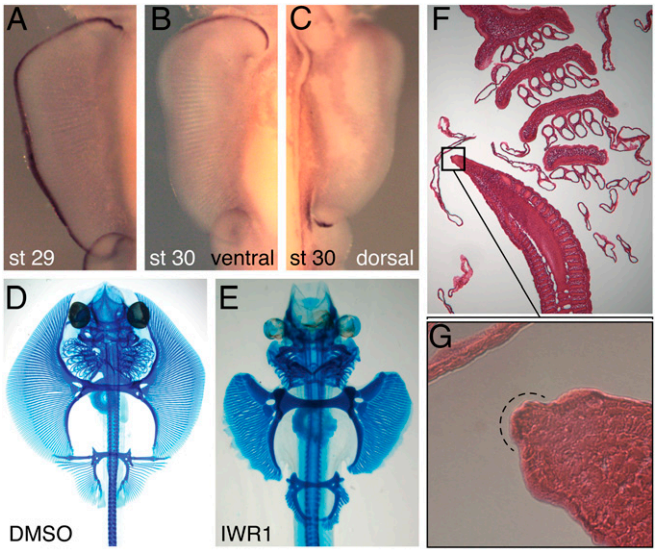

Fig. 3. Dual AERs in the developing paired fins of skates. (*A*–*C*) *Wnt3* expression in the pectoral fin of skate at stage 29 (*A*) and 30 (*B*, ventral view; *C*, dorsal view). *Wnt3* expression is a continuous strip in the ectoderm at stage 29, but splits into the anterior and posterior domain after stage 30. (*D* and *E*) Alcian Blue-stained skeletal preparations of skate embryos treated by DMSO or the WNT inhibitor IWR1. Pro- and mesopterygium were affected and shorter in IWR1-treated embryos compared with the control embryo. (*F* and *G*) Sagittal section of skate embryo at stage 30. An AER-like structure can be observed at the anterior tip of the pectoral fin (*G*).

of cyclopamine-treated embryos (*SI Appendix*, Fig. S9*D*) and found that ectopic expression of *Hoxa2b* rescued *Wnt3a* expression in 4 of the 24 embryos, implying that *3′Hox* genes have an ability to induce an AER marker gene (*SI Appendix*, Fig. S9*E*). However, more rigorous tests, such as establishing stable transgenic lines that may rescue *Wnt3a* expression efficiently, would strengthen this result.

As *5′Hox* genes maintain the AER in tetrapod limbs via an induction of *Fgf10* expression (24), *3′Hox* genes are likely to maintain the AER-like tissue of skate fins via *Fgf* genes in the anterior mesenchyme. In the skate pectoral fin, *Fgf7* is expressed highly in the anterior mesenchyme, especially underlying the anterior AER-like tissue at stage 30. This expression becomes gradually restricted to a narrow mesenchymal strip at stage 31 (Fig. 4 *F* and *G* and *SI Appendix*, Fig. S4). To test the function of *Fgf7* in skate fin development, acryl beads soaked in human-FGF7 protein were implanted into the mesenchyme of the central fin at stage 30, where *Wnt3* expression has ceased. FGF7 beads induced *Wnt3* expression in the ectoderm surrounding the implanted beads (Fig. 4 *H* and *I*). By contrast, SU5402, a chemical inhibitor of FGF receptors, was injected directly into the anterior pectoral fin, which resulted in a loss of *Wnt3* expression and a malformation of the propterygium (Fig. 4 *J*–*M*). These data demonstrate that *3′Hox–Fgf7–Wnt3* genes comprise an anterior genetic module responsible for maintaining the anterior AER-like tissue, in turn driving the extreme elongation of the batoid pectoral fin.

***Gli3* Inversion and Implications for Fin Diversity.** Previous studies showed that *Gli3* mRNA, which is expressed in the anterior of tetrapod limbs and restricts *Shh* to the posterior (25, 26), is expressed throughout the catshark pectoral fin and posteriorly in the elephant shark pectoral fin (10). Surprisingly, our RNA-seq and in situ hybridization data show that *Gli3* is expressed in the posterior pectoral and dorsal fin but is anteriorly localized in the pelvic fin of skate (Figs. 2 *A* and *B* and 5 *A*–*C* and *SI Appendix*, Fig. S5). To assess the generality of this pattern, we performed in situ hybridization of *Gli3* in bamboo shark and zebrafish. *Gli3* is also more enriched in the posterior mesenchyme of the pectoral fin but not the anterior in the pelvic fin in both species (Fig. 5 *D* and *E* and *SI Appendix*, Figs. S6 and S10). Thus, the pectoral fins of elephant shark, bamboo shark, skate, and zebrafish show an inverted pattern of *Gli3* expression relative to tetrapods, whereas the pelvic fins exhibit the tetrapod condition.

Discussion

One mechanism by which skates obtain their unique pectoral fin morphology is via the development of the extra AER-like tissue in the anterior fin. The posterior AER in the fin is equivalent to the canonical AER of tetrapods, whereas the anterior AER-like tissue is likely to be formed and maintained via a *3′Hox–Fgf7–Wnt3* module (Fig. 5*F*). The maintenance of an anterior AER-like tissue may be a novel feature deployed in skates to achieve the broad wing-like fin that enabled undulatory swimming and a benthic life history in batoids. Intriguingly, both *3′Hox* and *Fgf7* genes are expressed in the proximal region of the tetrapod limb (Fig. 1*G*) (22, 27). Furthermore, *Fgf7* can induce *Fgf8*, the AER marker in chicken (28). This preexisting genetic network was likely coopted to promote the anterior pectoral fin outgrowth of the skate. As *Fgf7*, *Fgf10*, and *Fgf22* diverged from the same ancestral *Fgf10*-like gene and bind to FGF receptor 2 (29), it is likely that the downstream targets of these genes are the same in the anterior and posterior pectoral fin of the skate. Our data suggest a role for *3′Hox* genes in the induction of *Fgf7* in the anterior portion of the skate fin, akin to the *5′Hox* gene

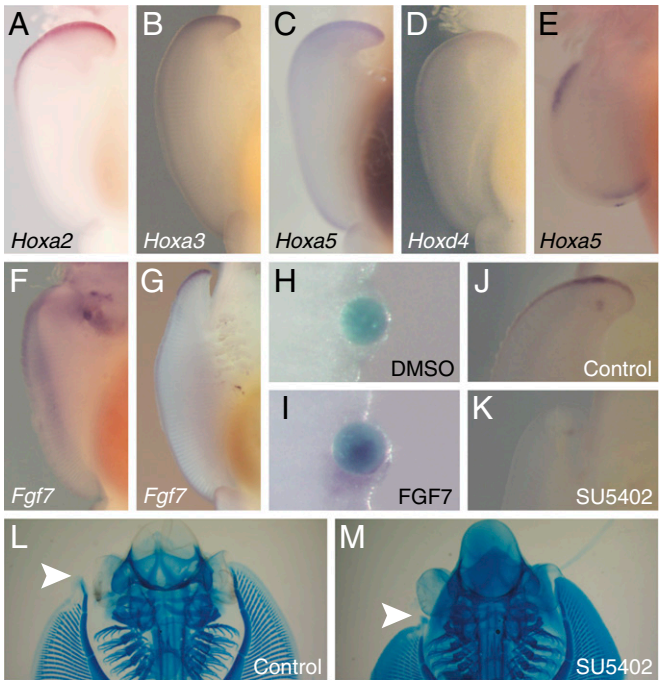

Fig. 4. An ancient genetic module underlies the pro- and mesopterygium. (*A*–*D*) The *3′Hox* gene expression patterns at stage 30. Each gene is expressed in the anterior mesenchyme. The expression domain is limited to only a narrow strip underlying the ectoderm. (*E*) *Hoxa5* in the pectoral fin of the shark (*C. plagiosum*), where expression is in the anterior and posterior fin mesenchyme. (*F* and *G*) *Fgf7* expression at stage 30 and 31. (*H* and *I*) *Wnt3* expression 1 d after the implantation of DMSO (*H*) or FGF7 beads (*I*). (*J* and *K*) *Wnt3* in situ hybridization in the pectoral fin at stage 31 following DMSO (*J*) or SU5402 (*K*) injection into the anterior fin. (*L* and *M*) Alcian Blue staining following DMSO or SU5402 injection into the anterior fin. The tip of the pectoral fin regressed in SU5402 injection (arrowheads).

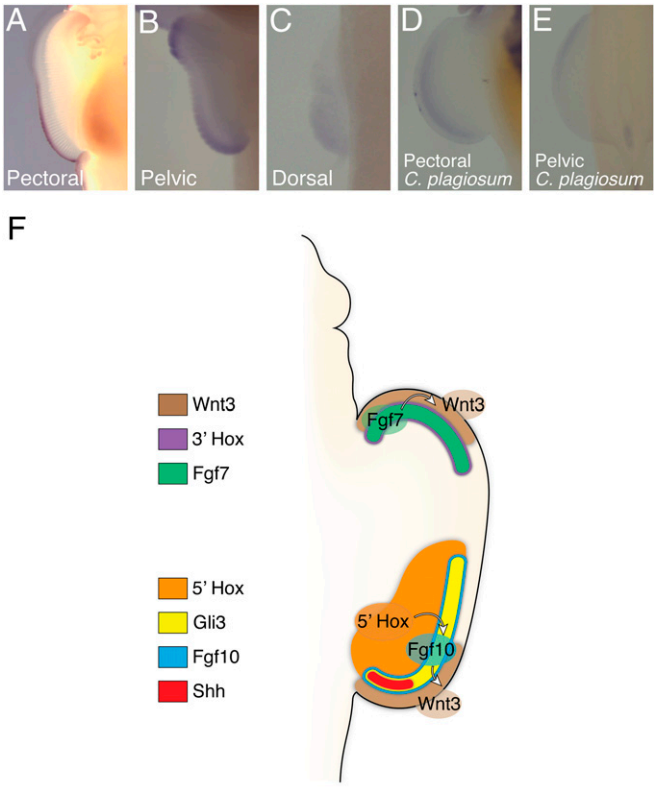

Fig. 5. *Gli3* expression inversion and the mechanism of skate fin development. (*A*–*C*) *Gli3* expression at stage 30 in the pectoral (*A*), pelvic (*B*), and dorsal fin (*C*) of skate. *Gli3* is expressed in the posterior side of the pectoral and dorsal fin while it is expressed in the anterior pelvic fin. The expression in the posterior tip of pelvic fin is likely in the clasper. (*D* and *E*) *Gli3* expression at stage 30 in the pectoral (*D*) or pelvic fin (*E*) of shark. *Gli3* is expressed in the posterior pectoral fin and in the anterior pelvic fin, as seen in skate. (*F*) Summary of molecular mechanisms controlling skate unique fin development. Although the posterior genetic module is similar to that of tetrapods, the anterior genetic module is distinct. *Fgf7* and *3′Hox* genes are expressed in the anterior mesenchyme and induce *Wnt3* expression, resulting in an extra AER-like tissue in the anterior fin. The posterior AER and anterior AER-like tissue extend the fin in posterior and anterior directions. Note that *Gli3* is coexpressed with *Shh* and *5′Hox* in the posterior fin.

induction of *Fgf10* in the tetrapod limb bud. Additional work to determine the precise function and downstream targets of *3′Hox* genes will be important to understand the evolution of these pathways. Despite the similarity of the two genetic modules in the anterior and posterior fin, the distribution of *3′Hox* mRNA in the anterior fin is distinct compared with that of *5′Hox* in the posterior fin; *3′Hox* expression domains in the mesenchyme of the anterior fin are narrower than the posterior *5′Hox* expression. This difference might reflect the functional discrepancy between *3′Hox* and *5′Hox* genes or tissue-level differences that influences *3′Hox* expression in the anterior fin.

Intriguingly, *Wnt3* maintains the AER in mice, whereas *Wnt3a* does so in the chicken limb bud (16, 30, 31). Cartilaginous fishes, including skates and sharks, represent the ancestral, extant-jawed vertebrates (Fig. 1*A*), and our analysis shows that *Wnt3* is expressed in the AER of the skate, which suggests that *Wnt3* plays an ancestral role in AER maintenance. *Wnt3* and *Wnt3a* diverged in fishes before the origin of amniotes. The function of AER maintenance was probably reassigned to *Wnt3a* in avians instead of *Wnt3*, even though the functional difference of WNT3 and WNT3A in the limb development remains unclear. A more precise phylogenetic test of *Wnt3* and *Wnt3a* expression will reveal how the AER has been maintained in different lineages in evolution.

Our data provide evidence for the evolutionary and developmental mechanisms underlying the extraordinarily wide fin of batoids. Skates are not the only extant species of fish with wide fins. Angel sharks also show a unique fin skeleton with an independently altered propterygium similar to skate (32, 33). In addition, the hillstream loach (*Beaufortia kweichowensis*) also contains particularly wide proximal radials. Thus, it will be intriguing to investigate if the same genetic modules are used during fin development in these additional taxa or if distinct modules are deployed. As our data point to redeployments of conserved genetic modules, future work will concentrate on understanding the regulatory controls that may have been modified to drive these modules in new areas of the developing appendage. A phylogenetically diverse understanding of the regulatory elements activating key factors (including *Hox* and *Fgf* genes) will be instrumental in uncovering the specific genetic mechanisms responsible for the previously unidentified activity of these conserved pathways.

Materials and Methods

Animal Husbandry and Manipulation. All processes and protocols for experimental animals were approved by the University of Chicago Institutional Animal Care and Use Committee (IACUC). *L. erinacea* embryos were purchased from the Marine Resource Center of The Marine Biological Laboratory. Embryos were kept at 15 °C in reconstituted Instant Ocean (Aquarium systems) with 12 h light–dark cycles. For functional assays, egg shells were removed and embryos were transferred into a small container with 200 mL Instant Ocean containing DMSO or IWR-1 (100 μM). At stage 32, embryos were subjected to Alcian Blue staining. Alcian Blue-stained embryos were generated as previously described (34). Bead implantation was performed as with other model organisms. Briefly, blue beads soaked in DMSO or human FGF7 protein solution (50 μg/mL; R&D Systems) were implanted into the center of the pectoral fin of anesthetized embryos. After 2 d, embryos were fixed by 4% (wt/vol) paraformaldehyde (PFA) and subjected to in situ hybridization. In situ hybridization was performed as previously described (35), except for a 60° incubation for hybridizing the *Fgf7* probe. All sequences for RNA probes of in situ hybridization were registered as a part of the transcriptome in National Center for Biotechnology Information (NCBI). *Hoxa5* in situ hybridization of *C. plagiosum* was performed by a probe cloned from *Scyliorhinus rotifer*. For inhibitor assays, an injection of DMSO or SU5402 (20 mg/mL DMSO; Sigma-Aldrich) into the anterior tip of the pectoral fin was repeated three times with each 3-d interval at stage 31, followed by Alcian Blue staining.

C. plagiosum embryos were supplied from the Shedd aquarium in Chicago, IL. Embryos were fixed and subjected to in situ hybridization. In situ hybridization was performed as described previously (35).

Antibody Staining of Phosphorylated Histone H3. After fixation of embryos by 4% (wt/vol) PFA, embryos were washed with PBS containing 0.1% Triton X-100 (PBT) followed by incubation in blocking solution (made from blocking reagent; Perkin-Elmer). The solution was substituted with blocking solution containing primary antibody (06-570; Millipore) and incubated for 3 d. Next, embryos were washed by PBT 5 h and incubated with secondary antibody (A110-34; Invitrogen) for 3 d. Embryos were washed by PBT for 5 h, stained by DAPI, and observed by a confocal microscopy. Paraffin sections were prepared at 8 μM, and the antigen was retrieved by citric buffer warmed with a microwave. The staining procedure was the same as the whole body staining.

Characterization of Ortholog Genes. The annotation of the skate transcriptome can be found in *SI Appendix*. Skate *Wnt3*, *Fgf7*, and *Gli3* and bamboo shark *Gli3* were cloned from cDNA of stage 30 pectoral fin by reverse-transcriptase PCR and integrated into pCRII-TOPO vector (Invitrogen). After sequencing, each gene was characterized by molecular phylogenetic analysis with Bayesian analysis. A modified amino acid sequence alignment was provided by ClustalW2 and calculated by Phyml. The graphs were drawn by NJplot.

RNA-Seq. Total RNA was extracted from three biological replicates from two domains (anterior and posterior fin) of *L. erinacea* embryos at stages 29 and 30 and three domains (anterior, center, and posterior fin) at stage 31 by Qiagen RNeasy kit. RNA-seq libraries were generated using the TruSeq Stranded mRNA kit (Illumina). Libraries were multiplexed and 100-bp paired-end sequencing was conducted on an Illumina HiSeq2000 sequencer.

***Hoxa2b* Ectopic Expression in Zebrafish Embryos.** The ORF sequence of zebrafish *Hoxa2b* genes were amplified by PCR using Platinum Taq DNA Polymerase High Fidelity (Invitrogen) and swapped into EGFP sequence of the Gar Island1-EGFP/PXIG vector (23) by Cla1 and Age1 restriction enzyme sites. The injection of vector and Tol2 transposase into zebrafish fertilized eggs was performed as previously described (23). After the injection, a portion of the eggs were transferred into separate dishes and treated by Cyclopamine (200 μM; LC Laboratories) from 24–36 hpf. All embryos were fixed at 36 hpf by 4% (wt/vol) PFA and subjected to whole-mount in situ hybridization, as previously described (23).

ACKNOWLEDGMENTS. We thank Jonathan D. Gitlin, Andrew Latimer, Rebecca Thomason, David Remsen, Scott H. Bennett, and the Marine Resource Center of The Marine Biological Laboratory for the experimental space and husbandry of skate and sharks; Benjamin L. King (Mount Desert Island Laboratory) for sharing unpublished skate transcriptome information; Glen Randall and Ana Shulla (University of Chicago) for the cell culture space; John Westlund (University of Chicago) for the elegant illustrations in this paper; and Michael Coates, Justin Lemberg, Noritaka Adachi, and Darcy Ross (University of Chicago) for stimulating discussion. This work was supported by The Brinson Foundation and the University of Chicago Biological Sciences Division (to N.H.S.); a Japanese Society for the Promotion of Science (JSPS) Postdoctoral Fellowship for Research Abroad, Uehara Memorial Foundation Research Fellowship, and Marine Biological Laboratory Research Grant (to T.N.); National Science Foundation Grant IOS-1355057 (to J.K.); Graduate Assistance in Areas of National Need Grant P200A120178 (to J.P.); NIH Grant T32 HD055164 and National Science Foundation Doctoral Dissertation Improvement Grant 1311436 (to A.R.G.); Brazilian National Council for Scientific and Technological Development Grants 402754/2012-3 and 477658/2012-1 (to I.S.); and Institutional Development Awards of NIH P20GM103423 and P20GM104318.

1. Alfred Sherwood Romer (1949) *The Vertebrate Body* (WB Saunders, Philadelphia).
2. Nelson JS (2006) *Fishes of the World* (Wiley, New Jersey), 4th Ed.
3. Janvier P (1996) *Early Vertebrates* (Clarendon Press, Oxford).
4. Aschliman NC, et al. (2012) Body plan convergence in the evolution of skates and rays (Chondrichthyes: Batoidea). *Mol Phylogenet Evol* 63(1):28–42.
5. Maxwell EE, Fröbisch NB, Heppleston AC (2008) Variability and conservation in late chondrichthyan development: Ontogeny of the winter skate (Leucoraja ocellata). *Anat Rec (Hoboken)* 291(9):1079–1087.
6. Luer CA, Walsh CJ, Bodine AB, Wyffels JT (2007) Normal embryonic development in the clearnose skate, Raja eglanteria, with experimental observations on artificial insemination. *Environ Biol Fishes* 80(2-3):239–255.
7. Dahn RD, Davis MC, Pappano WN, Shubin NH (2007) Sonic hedgehog function in chondrichthyan fins and the evolution of appendage patterning. *Nature* 445(7125): 311–314.
8. O'Shaughnessy KL, Dahn RD, Cohn MJ (2015) Molecular development of chondrichthyan claspers and the evolution of copulatory organs. *Nat Commun* 6:6698.
9. Freitas R, Zhang G, Cohn MJ (2007) Biphasic Hoxd gene expression in shark paired fins reveals an ancient origin of the distal limb domain. *PLoS One* 2(8):e754.
10. Onimaru K, et al. (2015) A shift in anterior-posterior positional information underlies the fin-to-limb evolution. *eLife* 4, 10.7554/eLife.07048.
11. Takahashi M, et al. (1998) The role of Alx-4 in the establishment of anteroposterior polarity during vertebrate limb development. *Development* 125(22):4417–4425.
12. LeClair EE, Bonfiglio L, Tuan RS (1999) Expression of the paired-box genes Pax-1 and Pax-9 in limb skeleton development. *Dev Dyn* 214(2):101–115.
13. Ohuchi H, et al. (1997) The mesenchymal factor, FGF10, initiates and maintains the outgrowth of the chick limb bud through interaction with FGF8, an apical ectodermal factor. *Development* 124(11):2235–2244.
14. Xu X, et al. (1998) Fibroblast growth factor receptor 2 (FGFR2)-mediated reciprocal regulation loop between FGF8 and FGF10 is essential for limb induction. *Development* 125(4):753–765.
15. Fernandez-Teran M, Ros MA (2008) The Apical Ectodermal Ridge: Morphological aspects and signaling pathways. *Int J Dev Biol* 52(7):857–871.
16. Barrow JR, et al. (2003) Ectodermal Wnt3/beta-catenin signaling is required for the establishment and maintenance of the apical ectodermal ridge. *Genes Dev* 17(3): 394–409.
17. Boulet AM, Moon AM, Arenkiel BR, Capecchi MR (2004) The roles of Fgf4 and Fgf8 in limb bud initiation and outgrowth. *Dev Biol* 273(2):361–372.
18. Moon AM, Capecchi MR (2000) Fgf8 is required for outgrowth and patterning of the limbs. *Nat Genet* 26(4):455–459.
19. Lewandoski M, Sun X, Martin GR (2000) Fgf8 signalling from the AER is essential for normal limb development. *Nat Genet* 26(4):460–463.
20. Maatouk DM, Choi K-S, Bouldin CM, Harfe BD (2009) In the limb AER Bmp2 and Bmp4 are required for dorsal-ventral patterning and interdigital cell death but not limb outgrowth. *Dev Biol* 327(2):516–523.
21. Chen B, et al. (2009) Small molecule-mediated disruption of Wnt-dependent signaling in tissue regeneration and cancer. *Nat Chem Biol* 5(2):100–107.
22. Zakany J, Duboule D (2007) The role of Hox genes during vertebrate limb development. *Curr Opin Genet Dev* 17(4):359–366.
23. Gehrke AR, et al. (2015) Deep conservation of wrist and digit enhancers in fish. *Proc Natl Acad Sci USA* 112(3):803–808.
24. Sheth R, et al. (2013) Decoupling the function of Hox and Shh in developing limb reveals multiple inputs of Hox genes on limb growth. *Development* 140(10): 2130–2138.
25. Litingtung Y, Dahn RD, Li Y, Fallon JF, Chiang C (2002) Shh and Gli3 are dispensable for limb skeleton formation but regulate digit number and identity. *Nature* 418(6901):979–983.
26. Te Welscher P, et al. (2002) Progression of vertebrate limb development through SHH-mediated counteraction of GLI3. *Science* 298(5594):827–830.
27. Kumar M, Chapman SC (2012) Cloning and expression analysis of Fgf5, 6 and 7 during early chick development. *Gene Expr Patterns* 12(7-8):245–253.
28. Yonei-Tamura S, et al. (1999) FGF7 and FGF10 directly induce the apical ectodermal ridge in chick embryos. *Dev Biol* 211(1):133–143.
29. Itoh N, Ornitz DM (2008) Functional evolutionary history of the mouse Fgf gene family. *Dev Dyn* 237(1):18–27.
30. Kengaku M, et al. (1998) Distinct WNT pathways regulating AER formation and dorsoventral polarity in the chick limb bud. *Science* 280(5367):1274–1277.
31. Narita T, Nishimatsu S, Wada N, Nohno T (2007) A Wnt3a variant participates in chick apical ectodermal ridge formation: Distinct biological activities of Wnt3a splice variants in chick limb development. *Dev Growth Differ* 49(6):493–501.
32. Stensio E (1959) *On the Pectoral Fin and Shoulder Girdle of the Arthrodires*, Kungl. Svenska Vetenskapsakademiens Handlingar, 4 ser (Almqvist & Wiksell, Stockholm).
33. de Carvalho MR, Kriwet J, Thies D (2008) A systematic and anatomical revision of Late Jurassic angelsharks (Chondrichthyes: Squatinidae). *Mesozoic Fishes 4 - Homol Phylogeny* 469–502.
34. Davis MC, Shubin NH, Force A (2004) Pectoral fin and girdle development in the basal actinopterygians Polyodon spathula and Acipenser transmontanus. *J Morphol* 262(2): 608–628.
35. Tanaka M, et al. (2002) Fin development in a cartilaginous fish and the origin of vertebrate limbs. *Nature* 416(6880):527–531.
36. Lee RTH, Thiery JP, Carney TJ (2013) Dermal fin rays and scales derive from mesoderm, not neural crest. *Curr Biol* 23(9):R336–R337.